

Rotor Dynamic Analysis for a Shaft Train by Using Finite Element Method

M. Najafi

Abstract—In the present paper, a large turbo-generator shaft train including a heavy-duty gas turbine engine, a coupling, and a generator is established. The method of analysis is based on finite element simplified model for lateral and torsional vibration calculation. The basic elements of rotor are the shafts and the disks which are represented as circular cross section flexible beams and rigid body elements, respectively. For more accurate results, the gyroscopic effect and bearing dynamics coefficients and function of rotation are taken into account, and for the influence of shear effect, rotor has been modeled in the form of Timoshenko beam. Lateral critical speeds, critical speed map, damped mode shapes, Campbell diagram, zones of instability, amplitudes, phase angles response due to synchronous forces of excitation and amplification factor are calculated. Also, in the present paper, the effect of imbalanced rotor and effects of changing in internal force and temperature are studied.

Keywords—Rotor dynamic analysis, Finite element method, shaft train, Campbell diagram.

I. INTRODUCTION

THE rotor and bearing system is one of the most important machine components used in many industrial machines such as turbines, compressors, and aircraft engines. At high rotational speed machines such as gas turbine, it is necessary to accurately predict the dynamic behavior of rotor to avoid of oscillation of system during operation for extending the lifetime of the machine. One of useful methods for recognizing this behavior is rotor dynamic analysis which has benefits in design phases and diagnosis process [1].

In 1895, the first idealized rotor system model consisting of circular section rotor with one disk in the middle of it, was proposed by Föppl. This model was employed by Jeffcott, in 1919 and thereafter this model called Jeffcott rotor or de Laval in Europe. Nowadays, Finite Element Method is the most prevalent method used today for rotor dynamics analysis [2]. For this investigation, a comprehensive in-house finite element code including different modules has been developed, and results have been compared with the plots of actual system. These conclusions would provide a reference for development of the machine and can be used as a powerful tool for fault diagnosis [3].

II. DIVISION OF ROTOR INTO DISCRETE SECTIONS

For preparing a discrete model of rotor system, the system should be divided into series of elements. These elements are in form of beam, disk, and supporting component. The beam element is contributing to the bending stiffness of the rotor, is

M. Najafi is with the Department of Mechanical Engineering, Tarbiat Modares University, Tehran, Iran (e-mail: majafae@gmail.com).

defined at first and end steps of axis symmetric cross section, and the disk element is associated with external mass and inertial loading. There are some guide lines mentioned in API to acquire sufficient resolution in model and to prevent numerical solution problems [4].

In order to define equivalent model for complex sections, bending analysis has been done in FEA codes, and for non-axis symmetric shaft, like generator, the equivalent section is calculated by:

$$R_1 = \sqrt{\frac{A-B}{2}}, \quad R_2 = \sqrt{\frac{A+B}{2}} \quad (1)$$

$$A = \frac{2I_{yy}}{m}, \quad B = \frac{m}{\rho\pi L} \quad (2)$$

Beam element has two nodes and four degrees of freedom (DOFs) in each one, and disk contains one node, mass and inertia properties are added to corresponding node [5].

Supporting elements include bearings and pedestals. In this system, fluid film bearings are represented by stiffness and damping characteristics function of rotational speeds which are added into bearing nodes. These characteristics are interpolated from database which has been already calculated from the FDM code. In the presented model, pedestals have steady characteristics particularly linear stiffness calculated by the FEM analysis. For sufficient accuracy, the mass of pedestal has been considered as well [6].

For this investigation, rotor system contains both gas turbine and generator's rotor, and for torque transmission an intermediate shaft has been used for direct coupling. The design philosophy of this component is based on isolating turbine rotor from generator malfunctioned torsional torque and standing against lateral vibration. The rotor system specification is listed in Table I.

TABLE I
THE ROTOR SYSTEM SPECIFICATION

	Length (m)	Weight (Ton)	Moment of Inertia (kg-m ²)
Turbine rotor	9.4	49.5	1600
Intermediate shaft	4.8	6	250
Generator Shaft	10.1	41	5500
Total	24.3	96	7350

The model consists of 149 nodes and four bearings and pedestal. Total DOF of model is 604 therefore. The four bearings are defined by geometrical dimensions like journal diameters, L/D, clearance, assembly clearance and oil

properties. For more accuracy in calculation, the effects of pedestal are considered. Pedestals are determined by mass and stiffness independent to rotational speed.

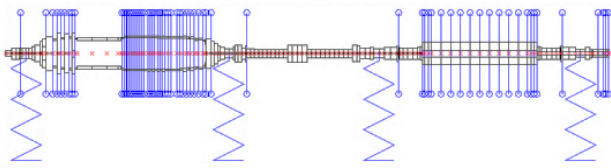


Fig. 1 Discrete model of rotor system and bearings

III. EQUATIONS OF MOTION

For this model, general equations are employed to represent inertia force, stiffness and damping forces, external exciting load and constant radial load in anisotropic rotor to reflect actual rotor mechanics better [7].

$$M \ddot{\delta} + C \dot{\delta} + K \delta = F(t) + P \quad (3)$$

The element matrices are eight orders represented for displacement and four slopes. The nodal vector is mentioned below and matrices of classic mass, inertial loaded, shaft stiffness, stiffness due to axial load and damping represents gyroscopic effect for lateral vibration are respectively mentioned.

$$M_1 = \frac{\rho A L}{420} \begin{bmatrix} 156 & 0 & 0 & -22L & 54 & 0 & 0 & 13L \\ 0 & 156 & 22L & 0 & 0 & 54 & -13L & 0 \\ 0 & 22L & 4L^2 & 0 & 0 & 13L & -3L^2 & 0 \\ -22L & 0 & 0 & 4L^2 & -13L & 0 & 0 & -3L^2 \\ 54 & 0 & 0 & -13L & 156 & 0 & 0 & 22L \\ 0 & 54 & 13L & 0 & 0 & 156 & -22L & 0 \\ 0 & -13L & -3L^2 & 0 & 0 & -22L & 4L^2 & 0 \\ 13L & 0 & 0 & -L^2 & 22L & 0 & 0 & 4L^2 \end{bmatrix} \quad (4)$$

$$M_2 = \frac{\rho I}{30L} \begin{bmatrix} 36 & 0 & 0 & -3L & -36 & 0 & 0 & -3L \\ 0 & 36 & 3L & 0 & 0 & 36 & -3L & 0 \\ 0 & 3L & 4L^2 & 0 & 0 & -3L & -L^2 & 0 \\ -3L & 0 & 0 & 4L^2 & 3L & 0 & 0 & -L^2 \\ -36 & 0 & 0 & 3L & 36 & 0 & 0 & 3L \\ 0 & -36 & -3L & 0 & 0 & 36 & -3L & 0 \\ 0 & 3L & -L^2 & 0 & 0 & -3L & 4L^2 & 0 \\ -3L & 0 & 0 & -L^2 & 3L & 0 & 0 & 4L^2 \end{bmatrix} \quad (5)$$

$$K_C = \frac{E}{(1+\alpha)L^3} \begin{bmatrix} 12 & 0 & 0 & -6L & -12 & 0 & 0 & -6L \\ 0 & 12 & 6L & 0 & 0 & -12 & 6L & 0 \\ 0 & 6L & (4+\alpha)L^2 & 0 & 0 & -6L & (2-\alpha)L^2 & 0 \\ -6L & 0 & 0 & (4+\alpha)L^2 & 6L & 0 & 0 & (2-\alpha)L^2 \\ -12 & 0 & 0 & 6L & 12 & 0 & 0 & 6L \\ 0 & -12 & -6L & 0 & 0 & 156 & -22L & 0 \\ 0 & 6L & (2-\alpha)L^2 & 0 & 0 & -22L & 4L^2 & 0 \\ -6L & 0 & 0 & (2-\alpha)L^2 & 6L & 0 & 0 & 4L^2 \end{bmatrix} \quad (6)$$

$$K_p = \frac{F_{axial}}{30L} \begin{bmatrix} 36 & 0 & 0 & -3L & -36 & 0 & 0 & -3L \\ 0 & 36 & 3L & 0 & 0 & -36 & 3L & 0 \\ 0 & 3L & 4L^2 & 0 & 0 & -3L & -L^2 & 0 \\ -3L & 0 & 0 & 4L^2 & 3L & 0 & 0 & -L^2 \\ -36 & 0 & 0 & 3L & 36 & 0 & 0 & 3L \\ 0 & -36 & -3L & 0 & 0 & 36 & -3L & 0 \\ 0 & 3L & -L^2 & 0 & 0 & -3L & 4L^2 & 0 \\ -3L & 0 & 0 & -L^2 & 3L & 0 & 0 & 4L^2 \end{bmatrix} \quad (7)$$

$$C = \frac{\rho I \Omega}{15L} \begin{bmatrix} 0 & -36 & -3L & 0 & 0 & 36 & -3L & 0 \\ 36 & 0 & 0 & -3L & -36 & 0 & 0 & -3L \\ 3L & 0 & 0 & -4L^2 & -3L & 0 & 0 & L^2 \\ 0 & 3L & 4L^2 & 0 & 0 & -3L & -L^2 & 0 \\ 0 & 36 & 3L & 0 & 0 & -36 & 3L & 0 \\ -36 & 0 & 0 & 3L & 36 & 0 & 0 & 3L \\ 3L & 0 & 0 & L^2 & 3L & 0 & 0 & -4L^2 \\ 0 & 3L & -L^2 & 0 & 0 & 3L & 4L^2 & 0 \end{bmatrix} \quad (8)$$

For including stiffness and damping matrices of bearings and pedestals, the following method is deduced:

$$\begin{bmatrix} M_R & 0 \\ 0 & M_F \end{bmatrix} \begin{bmatrix} \ddot{\delta}_R \\ \ddot{\delta}_F \end{bmatrix} + \begin{bmatrix} D_R + D_S & -D_S \\ -D_S & D_S + D_F \end{bmatrix} \begin{bmatrix} \dot{\delta}_R \\ \dot{\delta}_F \end{bmatrix} + \begin{bmatrix} K_R + K_B & -K_B \\ -K_B & K_R + K_F \end{bmatrix} \begin{bmatrix} \delta_R \\ \delta_F \end{bmatrix} = \begin{bmatrix} W_R + F_R(t) \\ W_F \end{bmatrix} \quad (9)$$

Prediction of torsional vibrations in rotor system has been done in order to avoid frequency interference around operational speed. This activity is essential due to low damping and common malfunction of generator as short circuit and asynchrony. In order to extract the distributed inertia matrix, kinetic energy of beam with uniform cross section and linear shape function has been used. Inertia and stiffness matrix are defined as following, and damping effect is neglected. In the torsional vibration, bearing effects are not considered.

$$K = \frac{\pi G (D_2^4 - D_1^4)}{32L} \begin{bmatrix} 1 & -1 \\ -1 & 1 \end{bmatrix} \quad (10)$$

$$M = \begin{bmatrix} \frac{I}{3} & \frac{I}{6} \\ \frac{I}{6} & \frac{I}{3} \end{bmatrix} \quad (11)$$

IV. EIGEN AND UNBALANCE RESPONSE SOLUTIONS

The eigensolution is applied to determine natural frequency, mode shape, Campbell diagram, and instability zones. The equation without external force is [8]:

$$M \ddot{\delta} + C(\Omega) \dot{\delta} + K(\Omega) \delta = 0 \quad (12)$$

Substituting $\delta = \Delta e^{nt}$ in last equation, the eigensolution of the following equation has been done:

$$AX = \omega BX \quad (13)$$

$$A = \begin{bmatrix} 0 & M \\ M & C \end{bmatrix} \quad (14)$$

$$F = \begin{bmatrix} f \sin(\Omega t) \\ f \cos(\Omega t) \end{bmatrix} \quad (18)$$

$$B = \begin{bmatrix} M & 0 \\ 0 & -K \end{bmatrix} \quad (15)$$

One of the most common forces on rotor system is unbalanced due to the allowance of the residual unbalances. According to this analysis, the response of rotor system will be predicted passing through critical speed. And the acceptance criteria for this response are calculating amplification factor in critical speed. The response is calculated by [9], [10]:

$$\begin{bmatrix} R_S \\ R_C \end{bmatrix} = C^{-1} F \quad (16)$$

$$C = \begin{bmatrix} K - M \omega^2 & -\Omega C \\ \Omega C & K - M \omega^2 \end{bmatrix} \quad (17)$$

V. RESULTS

At first, the torsion analysis was done where the results are mentioned in Table II and Fig. 2 The first three torsional mode of rotor system. By surveying them, it is obvious that there is a safe margin from rotational speed of rotor. The static analysis was done for extracting the deflection of rotor system. These results are derived in determining of rotor sag line. The plot was shown in Fig. 3.

Critical speeds of rotor system were obtained by interfere of synchronous harmonic line with natural frequencies with foreword whirl. The corresponding modes are illustrated in TABLE IV-VI. The results are compared by experimental trends, and it shows that the critical speeds are the same of actual ones with a little error.

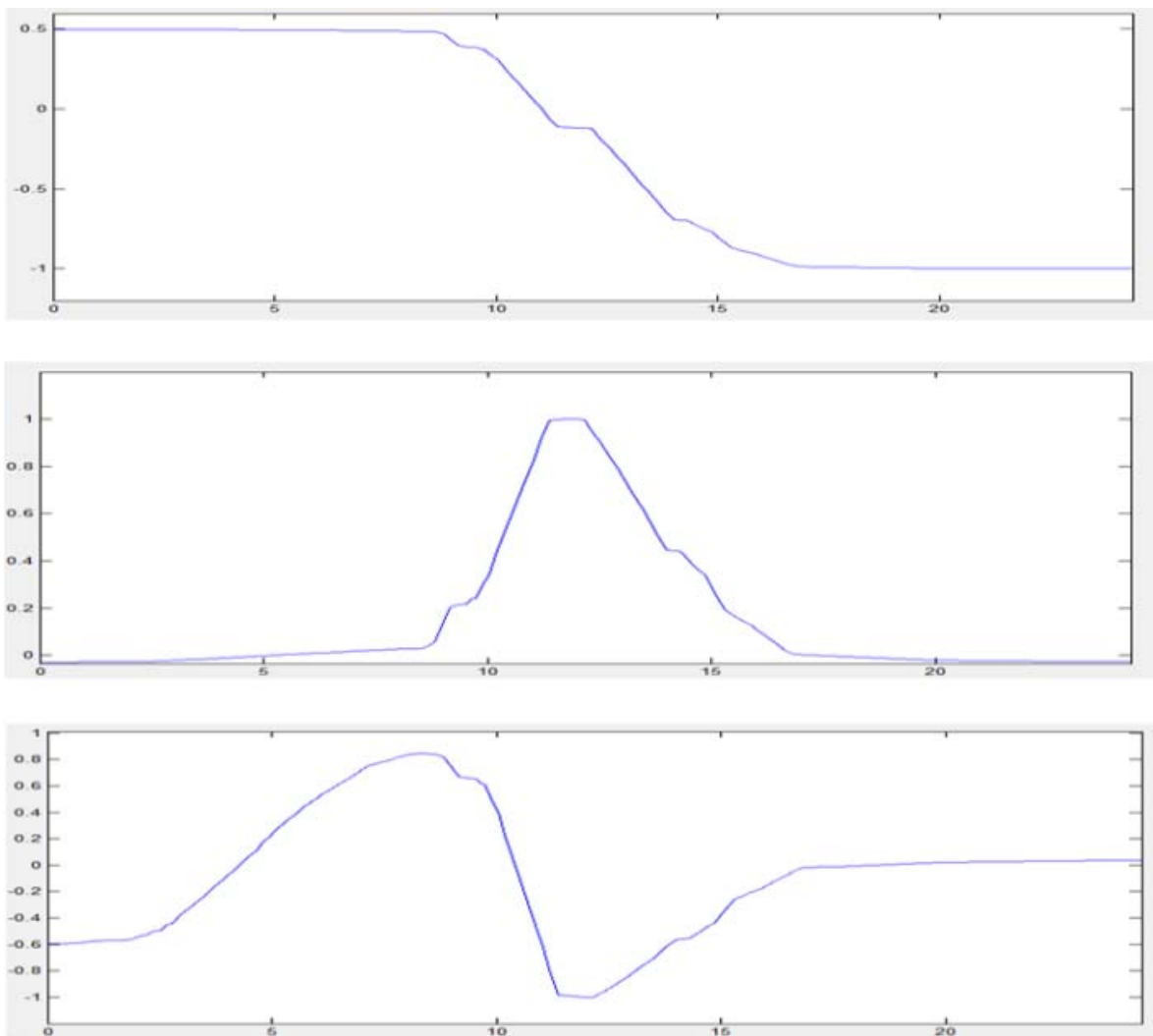


Fig. 2 The first three torsional mode of rotor system

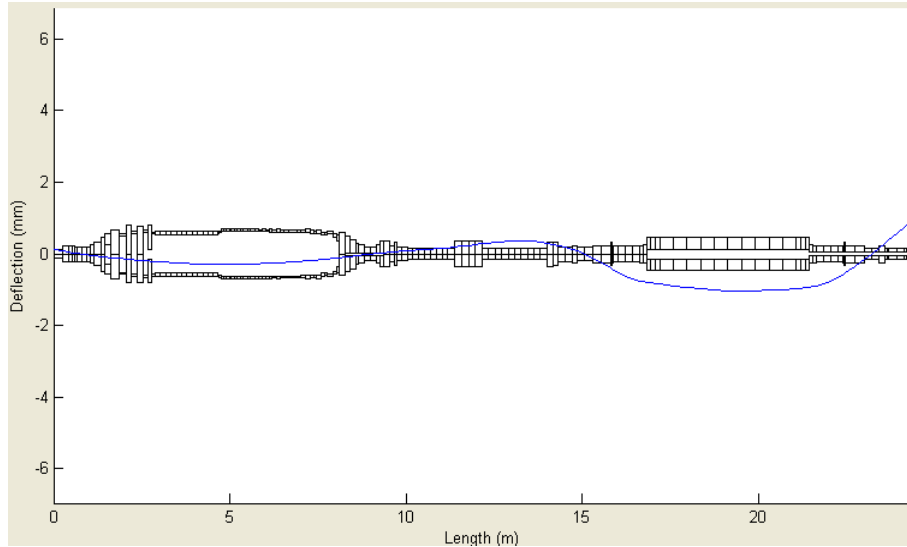


Fig. 3 Deflection of rotor system due to gravity

Campbell diagram is shown in Fig. 4, and it is very useful graph to predict any potential points for occurrence of rotor vibration due to any kind of external forces. For this system, there is a suitable margin around rotational speed.

For determining the instability speed of rotor system, eigensolution of rotor system, not subjected to external forces within operational speed, has been done. Unless the real part of Eigen value represented as viscous damping is negative, the system is unstable. This system becomes unstable in speed of 5000 rpm, which is 167% running speed.

1 st frq.	2 nd frq.	3 rd frq.	4 th frq.
10	108	138	193

13.8 Hz	25.4 Hz	40.4 Hz
14.4 Hz	28.3 Hz	58.5 Hz
16 Hz	31.6 Hz	65 Hz
24.6 Hz	35.8 Hz	72 Hz

TABLE IV
FLEXURAL MODES OF GENERATOR SIDE

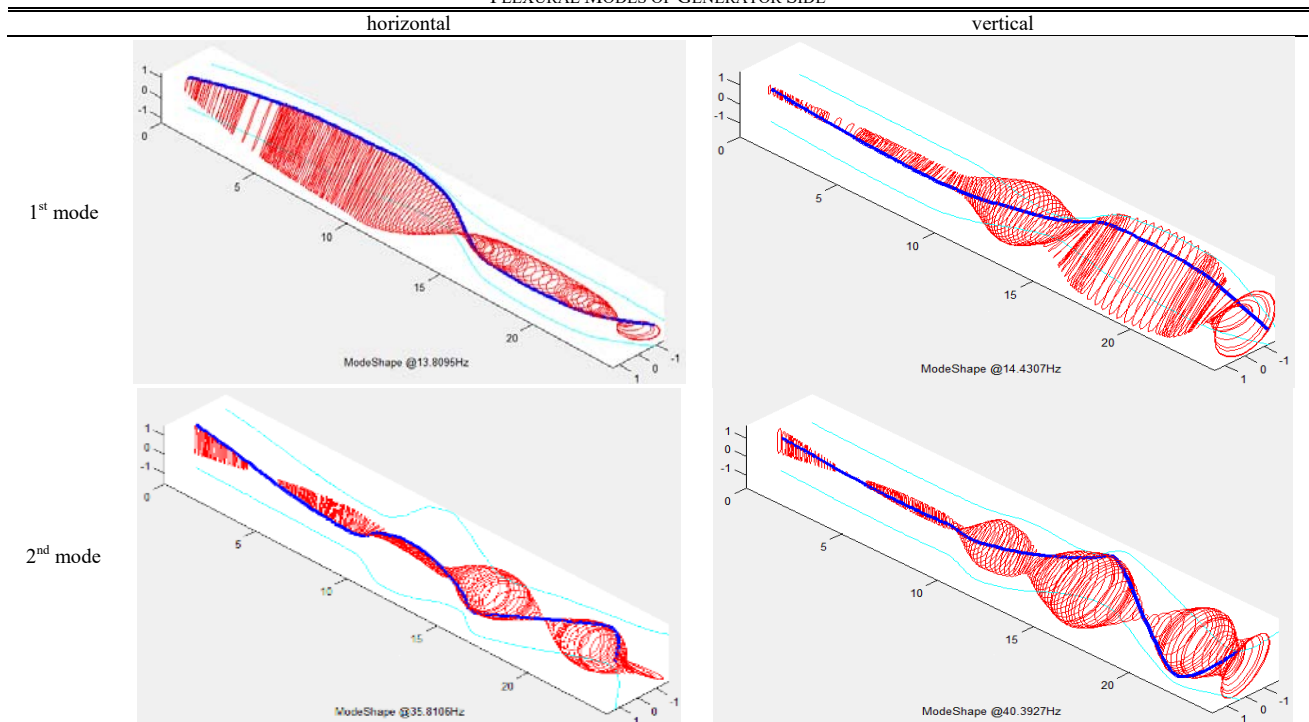


TABLE V
 FLEXURAL MODES OF TURBINE SIDE

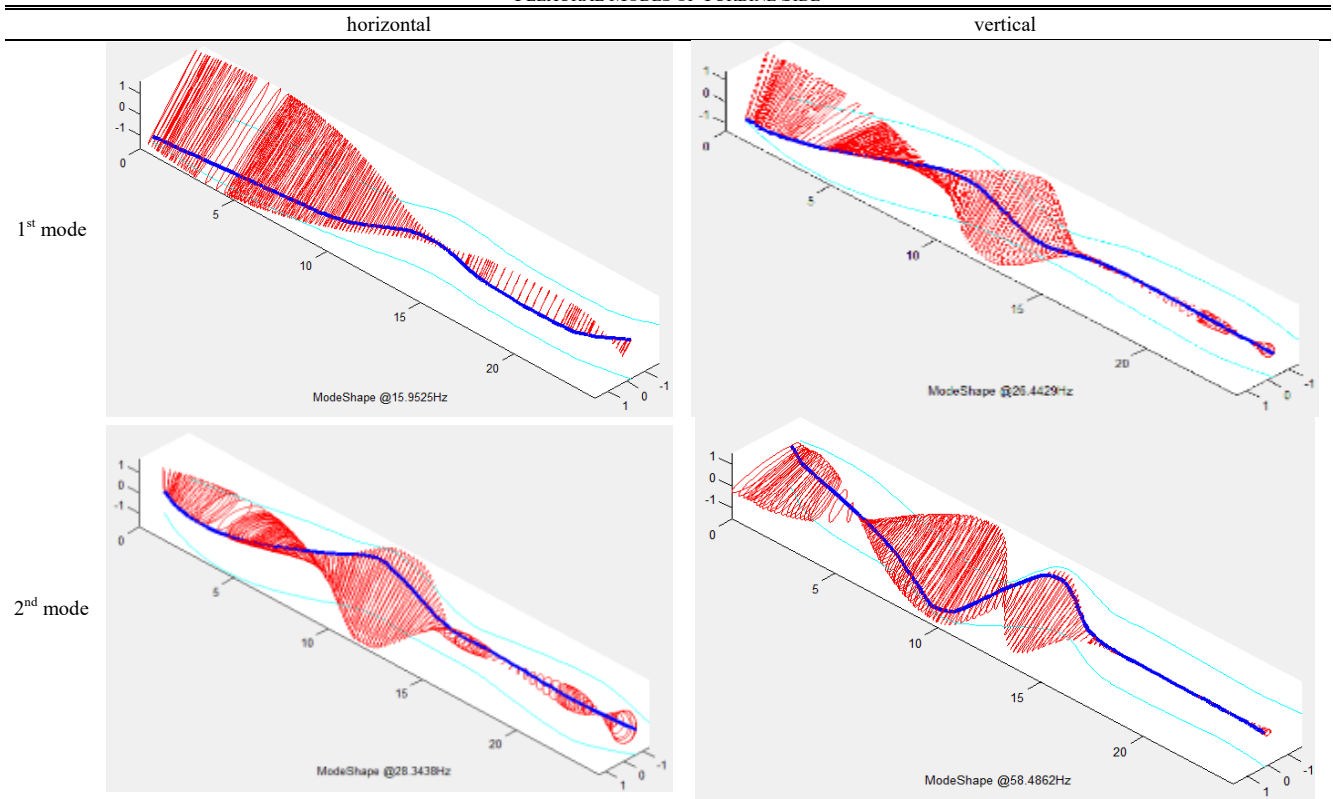
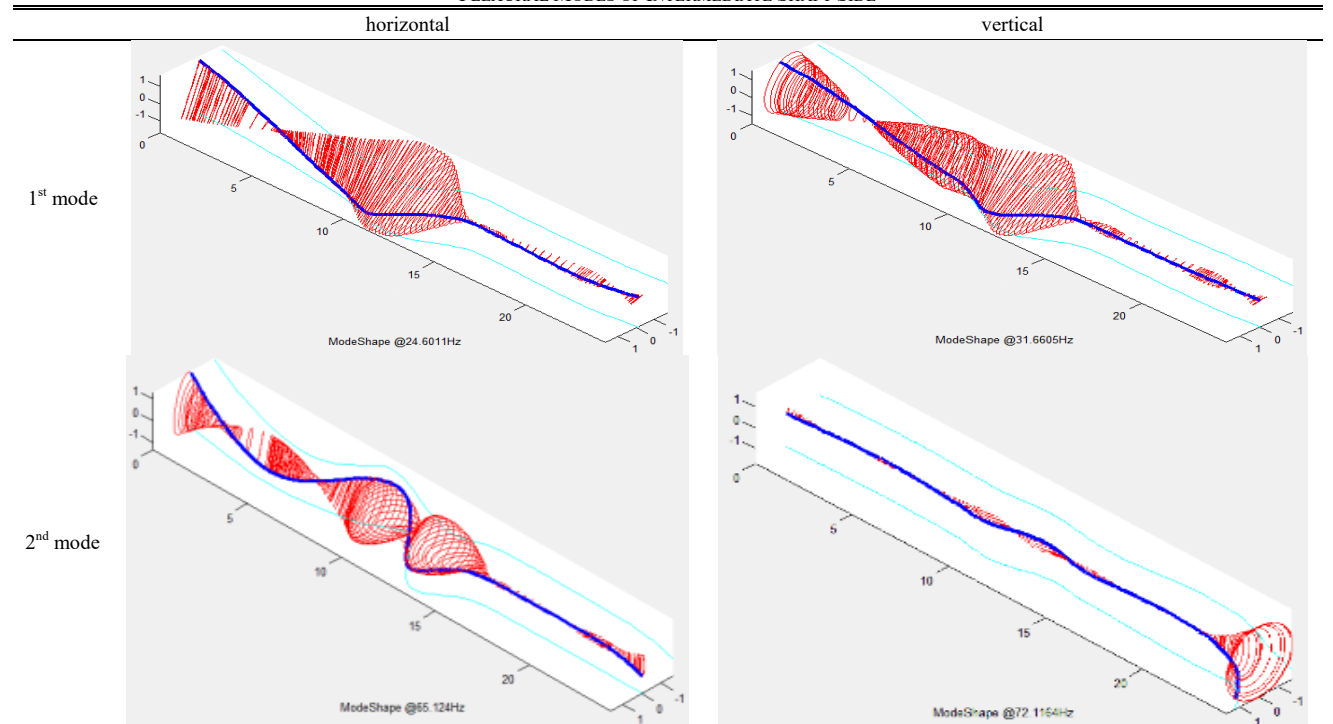


TABLE VI
 FLEXURAL MODES OF INTERMEDIATE SHAFT SIDE



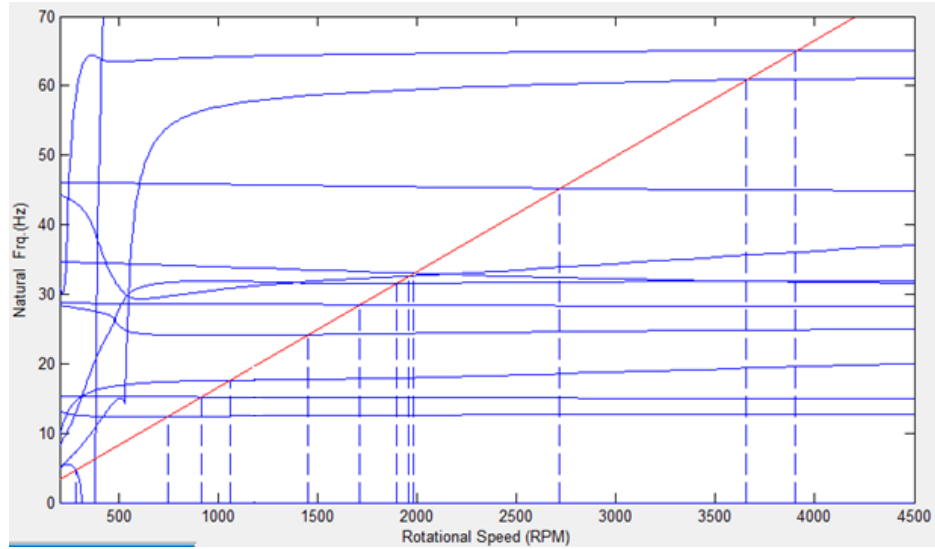


Fig. 4 Campbell diagram of rotor system

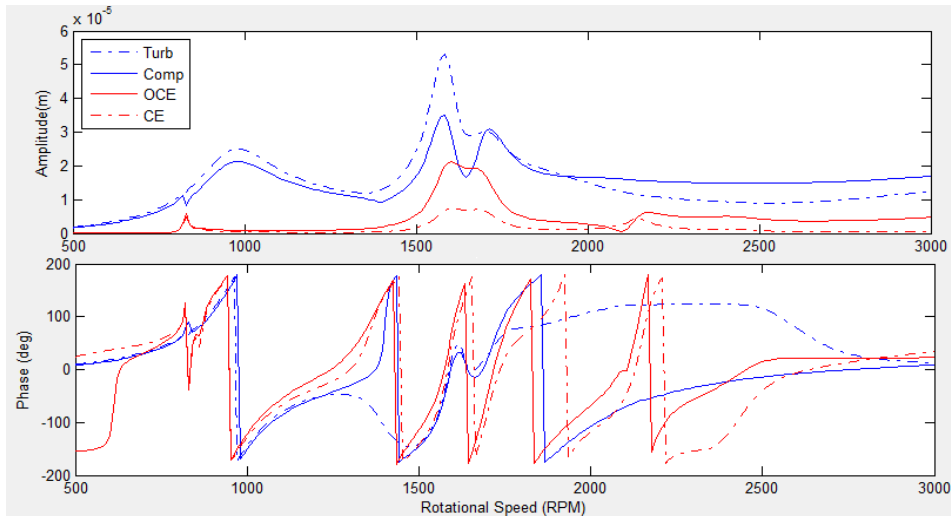


Fig. 5 Bode diagram for static UB in turbine section

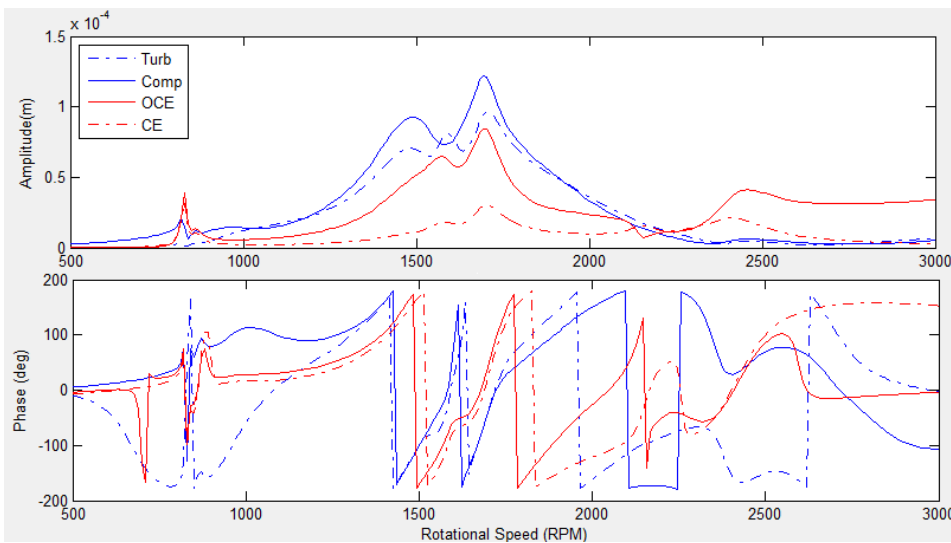


Fig. 6 Bode diagram for static UB in intermediate section

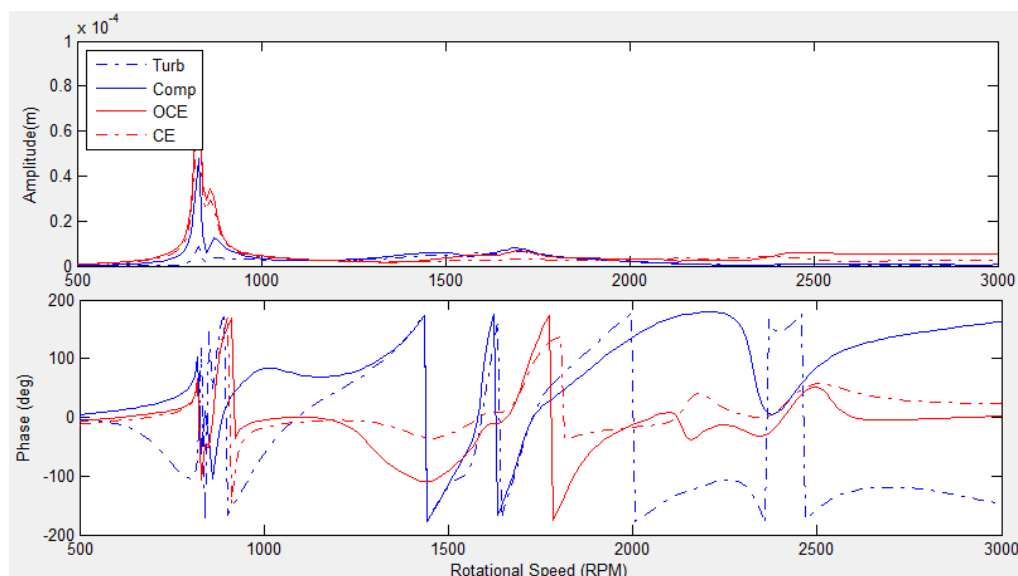


Fig. 7 Bode diagram for static UB in generator section

At the end, the unbalance responses of rotor system were obtained by inducing extra masses in different section of rotor system. The unbalance mass is selected according to ISO 1940 for G2.5. The results are illustrated in Fig. 5-7. These results show that the amplitude response of rotor is in allowable limit acc. to ISO7919-4 zones.

VI. CONCLUSION

A complete rotor dynamic analysis was conducted for a real shaft train of gas turbine plus generator by an in-house FEM based code. Torsional frequencies and critical speeds of rotor system and relative modes were obtained and compared with the real cases. The unbalance response analysis was conducted and results were compared with relative standard criteria. Campbell diagram was generated for predicting of excited frequencies.

REFERENCES

- [1] Y. Ishida, T. Yamamoto, Linear and Nonlinear Rotordynamic: A modern treatment with applications, Wiley, New York, 2012.
- [2] Michel Lalanne & Guy Ferraris, Rotordynamics Prediction in Engineering, 2nd ed. John Wiley and Sons.
- [3] L. Meirovitch, Fundamentals of Vibrations, McGraw Hill, New York, 2001.
- [4] G. Genta, Dynamics of Rotating Systems, Springer, New York, 2005.
- [5] Duncan Walker. Torsional Vibration of Turbo machinery, McGraw-hill.
- [6] Agnieszka Muszynska, Rotor dynamics, Taylor & Francis Group.
- [7] T. Someya, Journal Bearing Data book, Springer-Verlag.
- [8] API 684, Tutorial on the API Standard Paragraphs Covering Rotor Dynamics and Balancing
- [9] M Najafi, S Bab, F. Rahimi Dehgolan, Super Harmonic Nonlinear Lateral Vibration of an Axially Moving Beam with Rotating Prismatic Joint, World Academy of Science, Engineering and Technology, International Journal of Mechanical, Aerospace, Industrial, Mechatronic and Manufacturing Engineering Vol:11, No:4, 2017.
- [10] F. Rahimi Dehgolan, SE Khadem, S Bab, M Najafi, Linear Dynamic Stability Analysis of a Continuous Rotor-Disk-Blades System, World Academy of Science, Engineering and Technology, International Journal of Mechanical, Aerospace, Industrial, Mechatronic and Manufacturing Engineering, 12 (4) (2016) 349–357.